Individual differences in the mechanistic control of the dopaminergic midbrain

Lydia Hellrung[1*], Matthias Kirschner[2,3], James Sulzer[4], Ronald Sladky[2], Frank Scharnowski[2], Marcus Herdener[2], Philippe N. Tobler[1]

[1] Laboratory for Social and Neural Systems Research, Department of Economics, University of Zurich, Switzerland, University of Zurich, Zurich, Switzerland

[2] Center for Addictive Disorders, Psychiatric University Hospital, University of Zurich, Zurich, Switzerland

[3] Montreal Neurological Institute, McGill University, Montreal, Canada

[4] Department of Mechanical Engineering, University of Texas at Austin, Austin, USA

Corresponding author:

Lydia Hellrung, Laboratory for Social and Neural Systems Research, Department of Economics, University of Zurich, Blümlisalpstrasse 10, 8006 Zurich, Switzerland; E-mail: lydia.hellrung@econ.uzh.ch

Abstract

The dopaminergic midbrain is associated with elementary brain functions, such as reward processing, reinforcement learning, motivation and decision-making that are often disturbed in neuropsychiatric disease. Previous research has shown that activity in the dopaminergic midbrain can be endogenously modulated via neurofeedback, suggesting potential for non-pharmacological interventions. However, the robustness of endogenous modulation, a requirement for clinical translation, is unclear. Here, we used non-invasive modulation of the dopaminergic midbrain activity by real-time neurofeedback to examine how self-modulation capability affects transfer and correlated activation across the brain. In addition, to further elucidate potential mechanisms underlying successful self-regulation, we studied individual prediction error coding during neurofeedback training, and, during a completely independent monetary incentive delay (MID) task, individual reward sensitivity. Fifty-nine participants underwent neurofeedback training either in a veridical or inverted feedback group. Post-training activity within the cognitive control network was increased only in those individuals with successful self-regulation of the dopaminergic midbrain during neurofeedback training. Successful learning to regulate was accompanied by decreasing prefrontal prediction error signals and increased prefrontal reward sensitivity in the MID task. Our findings suggest that the cognitive control network contributes to successful transfer of the capability to upregulate the dopaminergic midbrain. The link of dopaminergic self-regulation with individual differences in prefrontal prediction error and reward sensitivity indicates that reinforcement learning contributes to successful top-down control of the midbrain. Our findings therefore provide new insights in the cognitive control of dopaminergic midbrain activity and pave the way to improving neurofeedback training in neuropsychiatric patients.

Keywords: real-time fMRI, neurofeedback, dopaminergic midbrain, substantia nigra, ventral tegmental area, dorsolateral prefrontal cortex, self-regulation, prediction error, reinforcement learning

1 Introduction

The dopaminergic midbrain, including the ventral tegmental area (VTA) and substantia nigra (SN), plays a crucial role in reward processing, reinforcement learning (Schultz, 2016, 1998; Tobler et al., 2007), motivation (Bromberg-Martin et al., 2010; Wise, 2004), and decision-making (Friston et al., 2014). Dysfunctions of the reward system have far-reaching consequences and are associated with the development of several severe psychiatric disease such as addiction (Huys et al., 2014) and schizophrenia (Deserno et al., 2016; Maia and Frank, 2017). Despite decades of extensive neuroscience and imaging studies which have contributed to an impressive body of knowledge of normal and abnormal reward system function, the neural mechanisms controlling midbrain activity are still not fully understood (Meder et al., 2019). One key issue that has received increasing attention over the last years is whether humans are able to cognitively control brain activity within the reward system. Although the mechanisms remained unclear, it has already been shown that both healthy controls (MacInnes et al., 2016; Sulzer et al., 2013b), and patients with cocaine addiction (Kirschner et al., 2018c) can learn to regulate SN/VTA activity during real-time functional magnetic resonance imaging (rt-fMRI) neurofeedback training. Yet, only little or no behavioral changes or increases in neural activity have been found so far to transfer beyond neurofeedback training, even though transfer, i.e., the ability to regulate activity also after training and without feedback is critical for clinical applications in disorders with reward system dysfunctions (Klein et al., 2019). The question therefore arises how individuals with successful transfer effects differ from individuals without transfer effects and what mechanisms underpin transfer effects. We narrowed this gap by combining data from two previous rt-fMRI studies (Kirschner et al., 2018c; Sulzer et al., 2013b) and pursuing three aims.

(1) Our first goal was to characterize individual differences in transfer effects between 'regulators' and 'non-regulators' in the context of SN/VTA self-regulation. Individual differences in regulation success and high variability of transfer effects arises also in other neurofeedback modalities such as electroencephalography (EEG) and are often neglected (Alkoby et al., 2018). For rt-fMRI

neurofeedback control, neural activity in the cognitive (or executive) control network may play an important role especially when performing a demanding task such as imagery (Sitaram et al., 2016). Therefore, and based on the known direct and indirect connections between prefrontal cortex and SN/VTA (Frankle et al., 2006; Gao et al., 2007; Sesack et al., 2003; Wu et al., 2013) we hypothesize that successful transfer of SN/VTA regulation is associated with activation in brain regions that are part of the cognitive (executive) control network, especially prefrontal areas.

(2) Our second goal was to determine whether mechanisms of (operant) associative learning can be used to explain neurofeedback training. In the associative learning framework of neurofeedback (Birbaumer et al., 2013; Sitaram et al., 2016), the chosen mental strategy is reinforced in proportion to the sign and magnitude of the feedback. If the feedback signal increases, reflecting a desired increase in brain activity within the target region, participants receive more reward than predicted corresponding to a positive prediction error. As a consequence, they would be more likely to repeat the strategy, expect higher feedback next time and gradually learn how to keep the feedback signal high. Accordingly, in regulators the size of the prediction error should gradually decrease as the expected feedback increasingly converges with the actual feedback. In contrast, for non-regulators and participants in a control group receiving unrelated or unstable feedback, the prediction errors would remain large and variable because these participants cannot learn any association between mental strategies and feedback. These straightforward implications of current theorizing about the mechanisms underlying neurofeedback remained largely untested (for a simulation study on the temporal dynamics of feedback: Oblak and colleagues (2017); for the correlation of BOLD with signal increase ('success') and decrease ('failure') during regulation: Radua and colleagues (2018)). Here, we directly investigate the prediction error mechanism in regions that control the SN/VTA, which itself has been traditionally associated with the coding of reward prediction errors (Schultz, 2016). Specifically, we hypothesize that decreasing prediction error signals during neurofeedback learning are associated with successful self-regulation and transfer effects.

(3) Our third aim was to identify individual differences in the ability to regulate the midbrain to general characteristics of the reward system, hoping to further distinguish regulators from non-regulators. Thus, we asked whether successful neurofeedback training (as measured by transfer effects) taps into general properties of the reward system. Given that adaptive reward processing characterizes the SN/VTA (Schultz, 1998; Tobler et al., 2005) we used a variant of the monetary incentive delay (MID) task that captures differences in adaptive reward sensitivity between clinical and non-clinical populations (Kirschner et al., 2018a). Using this task, we tested the hypothesis that reward processing in regions that may control the dopaminergic midbrain is related to successful SN/VTA self-regulation.

In sum, to study individual differences in capability to gain control of the SN/VTA we used rt-fMRI neurofeedback training in healthy participants receiving either real feedback (veridical group) or inverted feedback (control group). We quantified the individual degree of successful transfer by comparing the individual post-training versus pre-training self-regulation capabilities. Moreover, we related individual differences in reward sensitivity in separately measured SN/VTA self-regulation success.

2 Methods

2.1 Participants

Fifty-nine right-handed participants (45 males, average age 28.25±5.25 years) underwent neurofeedback training. We analysed data from two independent projects, which used highly similar rt-fMRI paradigms, rt-fMRI software and scanner hardware. The first dataset (Sulzer et al., 2013b) comprised male participants, randomly assigned to one of two groups. The experimental group received veridical neurofeedback (N = 15), the control group received inverted neurofeedback (N = 16) as training signal. The second dataset (Kirschner et al., 2018c) comprised the healthy control participants (N=28, 14 males) of a project investigating also cocaine users (these data are not presented here). This group received veridical neurofeedback. A subset of the participants in the

second dataset (N=25) also performed a variant of the monetary incentive delay (MID) task (Kirschner et al., 2018a). All participants provided written informed-consent and have been compensated for their participation. The Zurich cantonal ethics committee approved these studies in accordance with the Human Subjects Guidelines of the Declaration of Helsinki.

2.2 Experimental setup and neuroimaging

All participants underwent neuroimaging in a Philips Achieva 3 Tesla magnetic resonance (MR) scanner using an eight channel SENSE head coil (Philips, Best, The Netherlands) either at the Laboratory for Social and Neural Systems Research Zurich (SNS Lab, Study 1) or the MR Center of the Psychiatric Hospital of the University of Zurich (Study 2). First, we acquired anatomical images (Study1: gradient echo T1-weighted sequence in 301 sagittal plane slices of 250 × 250 mm^2 resulting in 1.1 mm^3 voxels; Study2: spin-echo T2-weighted sequence with 70 sagittal plane slices of 230 × 184 mm^2 resulting in 0.57 × 0.72 × 2 mm^3 voxel size) prior to neurofeedback training and loaded them into BrainVoyager QX v2.3 (Brain Innovation, Maastricht, The Netherlands) to identify SN/VTA as target region (see 2.4 for details). To acquire functional data, we used 27 ascending transversal slices in a gradient echo T2*-weighted whole brain echo-planar image sequence in both studies. The in-plane resolution was 2 × 2 mm^2, 3 mm slice thickness and 1.1 mm gap width over a field of view of 220 × 220 mm2, a TR/TE of 2000/35 ms and a flip angle of 82°. Slices were aligned with the anterior–posterior commissure and then tilted by 15°. Functional images were converted from Philips par/rec data format to ANALYZE and exported in real-time to the external analysis computer via the DRIN software library provided by Philips. This external computer ran Turbo BrainVoyager v3.0 (TBV – Brain Innovation, Maastricht, The Netherlands) to extract the BOLD signal from the images and calculate the neural activation for the feedback signal. The visual feedback signal was presented using custom-made software with Visual Studio 2008 (Microsoft, Redmond, WA, USA) through either a mirror mounted at the rear end of the scanner bore (Study 1) or through MR compatible goggles (Study 2).

2.3 Neurofeedback paradigm

The participants were instructed that their goal was to control a reward-related region-of-interest in their brains by imagining rewarding stimuli, actions, or events (note that we have previously shown that reward imagination activates SN/VTA with standard fMRI (Miyapuram et al., 2012)). Prior to scanning, we provided examples of such rewards, including palatable food items, motivating achievements, positive experiences with friends and family, favourite leisure activity or romantic imagery. We encouraged participants to use these different rewards as potential strategies for upregulating reward-related activity (during the cue 'Happy Time!', here referred to as IMAGINE_REWARD condition), which was fed back visually with a smiley vertically translating proportional to the SN/VTA BOLD signal (see below). In contrast, during the cue 'Rest' (here referred to as REST condition), participants were asked to perform neutral imagery, such as mental calculation to reduce reward-related activity. Prior to training, participants were familiarized with the 5s delay of the hemodynamic response affecting the display of the feedback and were asked not to move or change their breathing during the neurofeedback training.

Each neurofeedback session comprised: a pre-training imagery baseline run without any feedback, three (Study 1) or two (Study 2) training runs during which neurofeedback was presented (as Study 2 also investigated patients, training was limited to two runs), and a transfer run (i.e., without feedback). Each of these runs comprised nine blocks of IMAGINE_REWARD and REST conditions, each lasting 20 s. To determine the current level of the feedback signal we used the average of the last five volumes of the previous REST condition as reference value and employed a moving average of the previous three volumes to reduce noise. In the veridical feedback group, the smiley moved up with increasing percent signal change of SN/VTA BOLD signal and changed colour from red to yellow (Fig. 1 A). In the inverted feedback group, the smiley moved up and turned yellow with a decreasing SN/VTA BOLD signal.

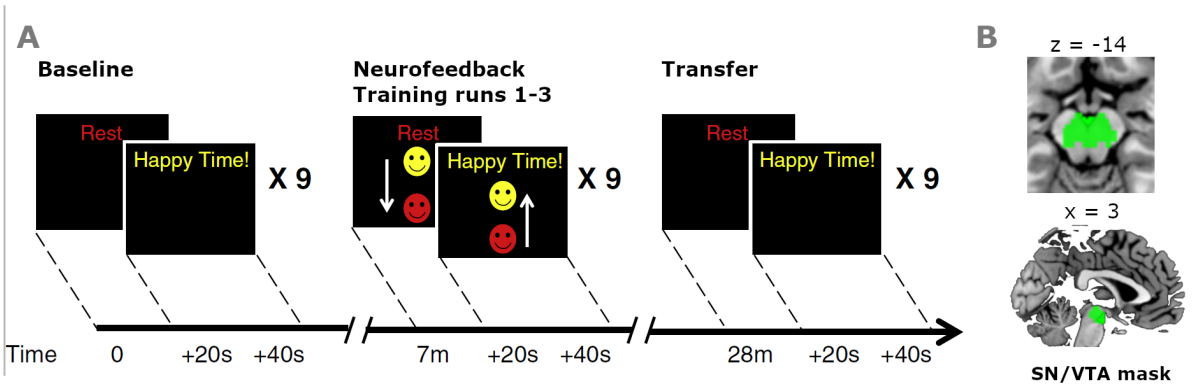

Figure 1 **Neurofeedback paradigm:** (A) All runs consisted of alternating blocks of REST and IMAGINE_REWARD conditions, with each block lasting 20 s. The regulation conditions (REST, IMAGINE_REWARD) were indicated by words ('Rest' or 'Happy Time!') and the feedback presented as moving smiley face during neurofeedback training runs. The preceding baseline and subsequent transfer runs comprised no feedback. The SN/VTA signal difference from these runs served to quantify the degree of regulation transfer (DORT) as ($SN/VTA_BOLD_{\{IMAGINE_REWARD,\ Transfer\}}$ - $SN/VTA_BOLD_{\{REST,\ Transfer\}}$) - ($SN/VTA_BOLD_{\{IMAGINE_REWARD,\ Baseline\}}$ - $SN/VTA_BOLD_{\{REST,\ Baseline\}}$). (B) Post-processed SN/VTA signal was extracted from the probabilistic atlas mask defined by Murty et al. (2014).

2.4 Region-of-interest SN/VTA

In both studies, the target region for neurofeedback, i.e. the substantia nigra (SN) and ventral tegmental area (VTA), was structurally identified using individual anatomical scans. Since the individual mask definition slightly differed between Study 1 and 2 (T1-weighted scans in Study 1 and T2-weighted scans in Study 2), we used an independent mask for our post-hoc analysis. By this, we can control for individual differences between experimenter ROI selection strategies, to avoid interpolation confounds due to warping by normalization and use a reliable seed region for functional connectivity analysis. The mask we are using here is a probabilistic mask of the SN and VTA as defined by (Murty et al., 2014), which is based on a large sample set (148 datasets) and available on https://www.adcocklab.org/neuroimaging-tools (download August 2018). Figure 1B illustrates this mask within the brain.

2.5 Degree of regulation transfer (DORT)

We assessed the effects of individual differences in performance to characterise participants in 'regulators' and 'non-regulators'. The measure of successful self-regulation was defined as individual degree of regulation transfer (DORT), i.e. as the condition-specific SN/VTA signal difference between post-training (Transfer) and pre-training (Baseline) runs:

$$DORT = (SN/VTA_BOLD_{\{IMAGINE_REWARD,Transfer\}} - SN/VTA_BOLD_{\{REST,Transfer\}}) - (SN/VTA_BOLD_{\{IMAGINE_REWARD,Baseline\}} - SN/VTA_BOLD_{\{REST,Baseline\}})$$

Thus, a positive DORT corresponds to a relative increase in post-training SN/VTA activity compared to pre-training SN/VTA activity for the contrast IMAGINE_REWARD minus REST. Please note that in these two runs (pre-training baseline, post-training transfer) no neurofeedback was presented. Thus to achieve positive transfer effects participants had to apply what they had learned during training runs.

DORT distributions: To investigate potential group differences in DORT, we transferred the extracted data to R (R-project R3.4.1). Using an anova, we tested for differences of the mean between the three groups (i.e. the two groups receiving veridical feedback in Studies 1 and 2 and the control group receiving inverted feedback in Study 1).

DORT in fMRI analysis: The DORT measure served to investigate the individual differences in successful transfer at the whole brain level. In particular, we were interested to identify regions that were positively associated with DORT and thus potentially contribute to regulation of the SN/VTA. For this analysis, we entered mean centered individual DORT levels in all fMRI second level statistical models (see 2.8). We excluded SN/VTA from all analyses to avoid any circularity.

Spatial specificity control analysis: To bolster the spatial specificity of our analysis about dopaminergic midbrain regulation, we additionally performed an analysis using the directly neighbored brain region of the parahippocampus as control target ROI. This target area is also active during the self-regulation task since the participants perform memory-based strategies. We extracted this mask from the wfu atlas and performed the identical main effects analysis as described above. To compare the results between our target ROI SN/VTA and control ROI in parahippocampus, we performed a conjunction analysis between the resulting contrast images. This comparison revealed only two common areas within the cerebellum and the Temporal Gyrus. The limited commonalities between these two target ROI's, especially in striatal and prefrontal areas, indicate the spatial specificity of our findings using the SN/VTA as target region (see Supplemental Material Figure S4 and Table S8).

2.6 MID Task

In every trial of the MID task (Kirschner et al., 2018b, 2016; Simon et al., 2015) first one of three cues appeared (Fig. S1). One cue was associated with large reward (ranging from 0 to 2.00 CHF), one cue with small reward (0 to 0.40 CHF) and one cue with no reward. After a delay of 2.5 to 3 s, participants had to identify an outlier from three circles by pressing one of three buttons as quickly as possible. Depending on the cue, their response time and the correctness of the answer, participants gained an amount of money. Importantly, the use of large and small reward ranges enables investigation of individual differences not only in general reward sensitivity but also in how well the reward system adapts to different reward distributions, so-called adaptive reward coding (Kirschner et al., 2018a).

2.7 MR Data pre-processing

We despiked the functional data using AFNI (http://afni.nimh.nih.gov/afni). To account for differences in EPI slice acquisition times we employed temporal interpolation of the MR signal, shifting the signal of the misaligned slices to the first slice (Sladky et al., 2011) using FSL 5 (FMRIB Software Library, Analysis Group, FMRIB, Oxford, http://fsl.fmrib.ox.ac.uk). Furthermore, data were bias-field corrected using ANTs (http://stnava.github.io/ANTs), realigned using FSL 5, normalized to standard MNI space using ANTs in combination with a custom scanner-specific EPI-template resulting in a 1.5 mm^3 isotropic resolution and finally smoothed with a 6 mm FWHM Gaussian kernel using FSL 5.

The spatial specificity control analyses (see Supplemental Material Figure S4 and Table S8) suggest that the data are not due to common physiological noise. To more directly account for noise, we additionally acquired physiological data in a subsample of participants. In the available subsample, neither changes in heart rate variability nor respiration were significantly correlated with VTA/SN activation during reward imagination (see details in Kirschner et al., 2018, Supplemental Material Table S1, Figure S1). Here, we also used an image-based correction to account for physiological artefacts in all participants. Since physiological artefacts are most prominently present in CSF and white matter due to the absence of BOLD effects, pulsations of the ventricles, and proximity to the large brain arteries (e.g., circle of Willis), we decided to use an established preprocessing procedure based on a

192 PCA approach (Sladky et al., 2013; Weissenbacher et al., 2009). Specifically, we calculated the global
193 mean and the first 6 components of a temporal principal component analysis on the cerebrospinal
194 fluid and white matter signal. These 6 components were used as noise regressors in the first level
195 statistics (see 2.8) in addition to the 6 motion parameters. Along with the pre-processing of the fMRI
196 data, the SN/VTA mask used as ROI for the analysis was resliced into the dimensions of the functional
197 data using SPM 12 (v6906, http://www.fil.ion.ucl.ac.uk/spm/software/spm12/) within Matlab R2016b
198 (www.mathworks.com).

199 **2.8 MR Data analysis**

200 For all of the following analyses, we used the toolbox SPM 12 (v6906) within Matlab R2016b. All figures
201 were created using bspmview v.20161108 (Spunt, 2016) and ggplot2 within R 3.4.1. All group-level
202 analysis included an additional covariate for the dataset to account for potential global signal
203 differences between studies.

204 2.8.1 Post-training effects: Correlation with DORT in veridical and inverted feedback group

205 The first question of this study asked whether the individual degree of successful neurofeedback
206 transfer is associated with individual differences in the cognitive control network. To answer this
207 question, we conducted a general linear model (GLM) on the single subject level including one block-
208 wise regressor for the IMAGINE_REWARD condition and one for the REST condition with 190 timesteps
209 (each condition comprised 9 onsets and lasted 20 s) for each of the four runs separately. Additionally,
210 we modelled the first 5 TRs of every run as nuisance regressor and added also motion and physiological
211 artefact regressors (see 2.7) in the design matrix. In total the GLM consisted of fifteen regressors. We
212 formed the contrast IMAGINE_REWARD-REST and compared it between Transfer and Baseline runs,
213 i.e. $(\text{IMAGINE_REWARD-REST})_{\text{Transfer}} - (\text{IMAGINE_REWARD-REST})_{\text{Baseline}}$. At the group level, we tested
214 for correlation of DORT with this contrast in a one-sample t-test. We ran these analyses separately for
215 both the veridical and inverted feedback groups. To test for common and separate activity between
216 the groups, we performed conjunction and disjunction analyses over the two group maps. Additionally,
217 we performed a two-sample t-test group comparison analysis to identify significant group differences.

To identify activity within the cognitive control network, we used a cognitive control template based on the coordinates from a meta-analysis (Niendam et al., 2012). We created this template with fslmaths and spheres of 15 mm around all coordinates from the meta-analysis. In table S1 we identify regions of the cognitive control network where transfer success correlates with DORT both within the template. For statistical maps, we used FWE-corrected cluster level threshold with $p < .05$ (cluster extent of 230 voxel) based on whole brain statistics $p < .001$. In addition, to test the functional specificity of our results, we performed a meta-analytic functional decoding analysis using the Neurosynth database (www.neurosynth.org). This relates the neural signatures of the cognitive control decoding network to other task-related neural patterns (Fig. S2).

2.8.2 Prediction error coding analysis during NF training

The second question of the study was to investigate whether successful neurofeedback performance was associated with a reduction in prediction error as assumed by a classic reinforcement learning mechanism. To address this issue specifically for the neurofeedback training runs we constructed a GLM that replaced the block (IMAGINE_REWARD and REST) regressors with corresponding event regressors that modelled every TR and that we parametrically modulated with a time-resolved continuous prediction error (PE) term. This PE term was defined as difference between the current and the previous TR within the SN/VTA mask, i.e. ($BOLD_SN/VTA_t$- $BOLD_SN/VTA_{t-1}$; accordingly, in the upregulation condition the parametric modulator corresponded to $IMAGINE_REWARD_t$ – $IMAGINE_REWARD_{t-1}$). To investigate if the prediction error decreases over time, we used the difference (parametric modulator PE (run 2) – parametric modulator PE (run 1), i.e. PE coding in neurofeedback training run 2 minus neurofeedback training run 1 (Figure 1A). This difference should become negative as prediction errors decrease with learning. On the group level, we correlated this contrast (difference in PE coding run2 – PE coding run1) with the DORT measure in a one-sample t-test to test for associations between a decrease in prediction error coding and successful self-regulation.

The results of this analysis, showing prediction error coding in the dorsolateral prefrontal cortex (dlPFC), inspired a functional connectivity analysis. Specifically, we investigated the functional

244 impact of the dlPFC prediction error signal on the SN/VTA using a psychophysiological interaction
245 analysis using the gPPI v13 Toolbox (McLaren et al., 2012) based on the MNI coordinate of dlPFC (x=40,
246 y=10, z=38) with a 5 mm sphere as seed region. We added activity from this seed region as
247 physiological regressor to the original GLM (2.7.2) and interacted it with both the IMAGINE_REWARD
248 and REST regressors to form interaction regressors. Functional connectivity was calculated by
249 contrasting the interaction terms IMAGINE_REWARD-REST between second and first neurofeedback
250 training run. We then correlated this contrast with DORT. The results were masked with the SN/VTA
251 mask for illustration purposes. For statistical maps, we used a whole-brain threshold of $p < .001$ (50
252 voxel extent).

253 2.8.3 Relation between DORT and reward sensitivity in the MID Task

254 To address the third aim of the study, we investigated the relationship between reward processing in
255 the MID task and the capacity to successfully regulate the SN/VTA in the neurofeedback experiment.
256 In particular, we considered two contrasts in the MID task (1) general reward sensitivity, defined as
257 the sum of parametric modulators: small plus large reward (2) adaptive reward coding, defined as the
258 difference between parametric modulators: small minus large reward. Again, we used correlation
259 analysis at the group level to determine whether these two contrasts are related with individual
260 transfer success (DORT) in the neurofeedback task. Moreover, to assess the commonalities of the
261 neural activities in these different tasks, we performed a conjunction analysis of contrasts (1), (2) and
262 the correlation of transfer-activity with DORT (see 2.8.1). For illustration purposes of this conjunction
263 analysis, we used a threshold of $p < .005$, for reporting we used $p < .001$ (cluster extent = 50).

264

265 **2.9 Additional behavioral measurements**

266 **Strategies:** All participants were introduced to five example strategies (see 2.3) that might be used to
267 up-regulate brain activity but also free to use their own strategies. At the end of the experiment,
268 participants filled in a custom-made questionnaire on the strategies they used. To compare strategies

between the groups, we used a χ2-test to assess differences in the distribution of strategy usage. We did not observe any significant group differences in strategy use (p = .9), and therefore did not consider this measurement in any further analysis.

Personality measures: To investigate whether individual differences in behavior and personality were associated with individual differences in DORT, Study 2 measured: (1) Smoking status in number of cigarettes per day; (2) verbal IQ as determined by the Multiple Word Test (MWT, Lehrl, 2005); (3) Positive and Negative Affect Score (PANAS) in the German version (Krohne et al., 1996); (4) attentional and nonplanning subscores of the Barratt Impulsivity Scale in the German version (Preuss et al., 2008). We tested for correlations with the DORT parameter using Pearson correlations. As none of these variables correlated significantly with the DORT parameter (all p > .5), we did not consider them further.

3 Results

3.1 No difference in degree of regulation transfer (DORT) across groups

We first evaluated the DORT measure and compared it between the three datasets. There were no significant differences across all three groups (mean veridical group Study 1 = .01, mean veridical group Study 2 = -.02, mean inverted group Study 1= -.05; F(2, 56) = .13; Fig. 1). Moreover, also the direct comparison between the two veridical groups was not significant (T(39) = -.26, *p* = .8). Accordingly, we combined the two veridical groups for subsequent analyses. Importantly, our participants showed considerable variation in DORT, which allowed us to investigate the individual differences in brain activity accompanying more or less successful regulation of the SN/VTA through neurofeedback. Thus,

289 the groups showed similar mean levels and considerable individual differences in self-regulation

290 success.

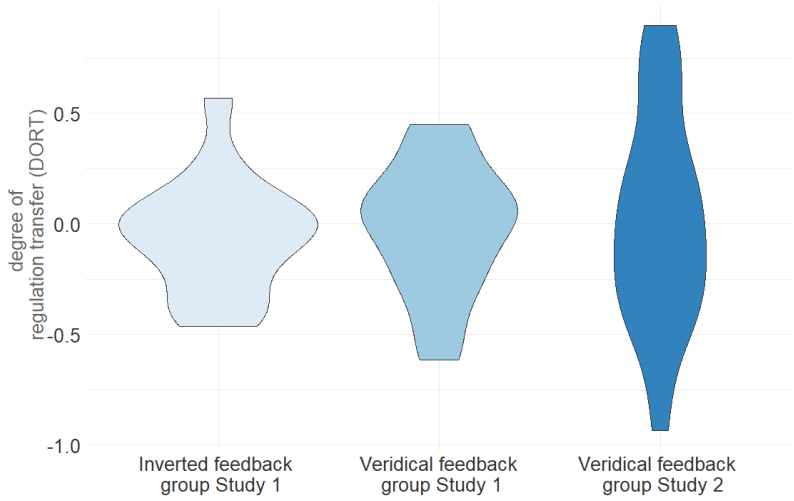

Figure 2 **Distribution of DORT across groups.** The DORT measure was distributed similarly in both groups receiving veridical feedback in Studies 1 and 2 and the control group receiving inverted feedback in Study 1. Accordingly, we found no evidence supporting a main effect of feedback on transfer. However, DORT varied substantially across individuals, which motivated the analyses using the individual self-regulation

291 **3.2 Individual variation in transfer: DORT associated with cognitive control network in**
292 **veridical and amygdala activity in inverted feedback group**

293 3.2.1 Veridical feedback group

294 We investigated whether individual levels of successful SN/VTA self-regulation (DORT) were associated

295 with increased post-training activity compared to pre-training activity $(\text{IMAGINE_REWARD-REST})_{\text{Transfer}}$

296 – $(\text{IMAGINE_REWARD-REST})_{\text{Baseline}}$). This analysis revealed several areas consistently reported by

297 neurofeedback studies (see Fig. 2 in the meta-analysis of Sitaram et al., 2016), including dorsolateral

298 prefrontal cortex (dlPFC), anterior cingulate cortex (ACC), lateral occipital cortex (LOC), and thalamus

299 (Figure 3A and Table 1). To formally test for a more general association with the cognitive control

300 network, we applied a cognitive control network template from a meta-analysis (Niendam et al., 2012),

301 which in addition revealed neural activity in precuneus and striatum (Fig. 3B for exemplary illustrations

of dlPFC, ACC, temporal gyrus, and thalamus activity; Table S1 for full overview). Thus, regions of the cognitive control network showed transfer to the extent that neurofeedback training of the dopaminergic midbrain was successful.

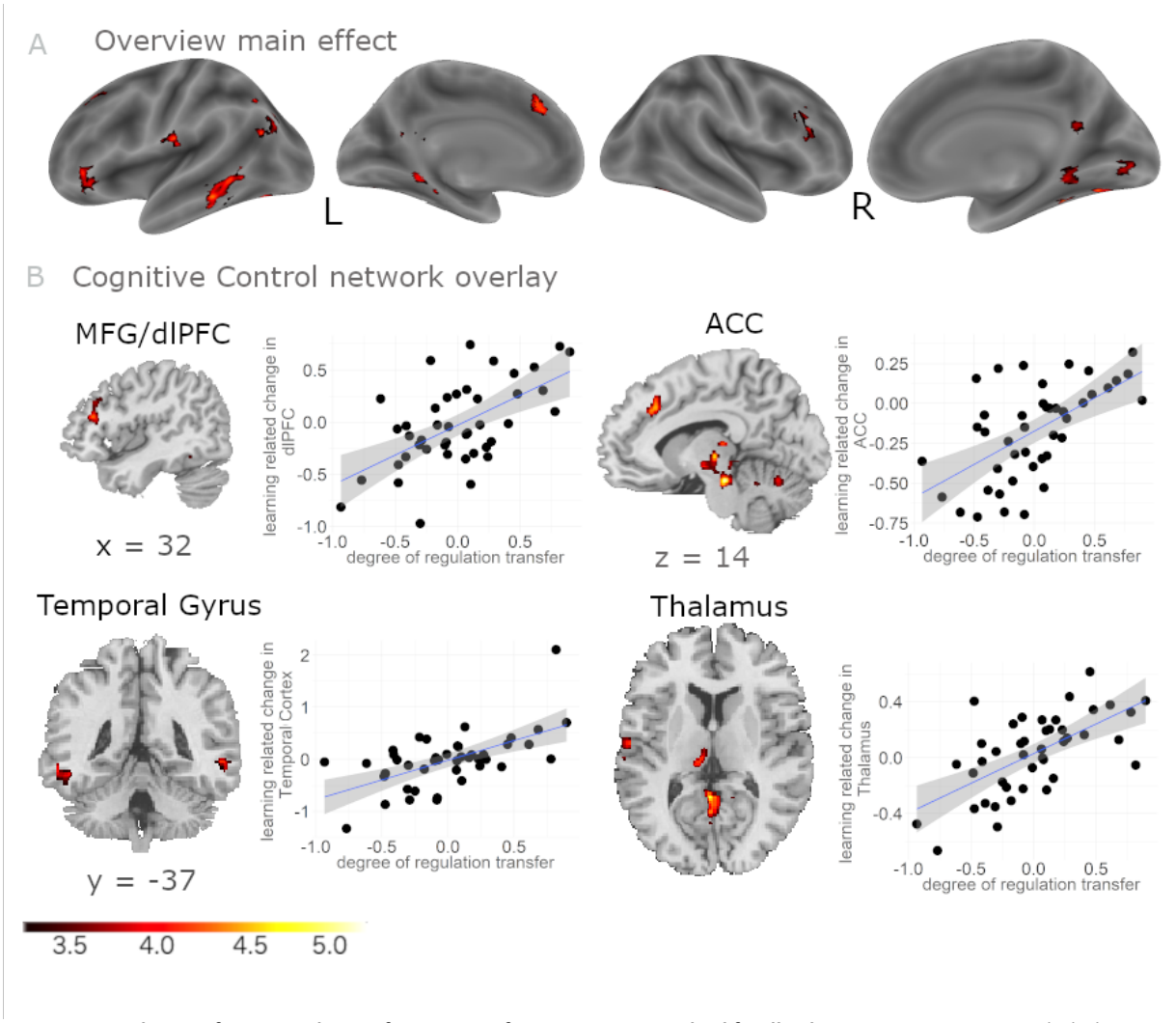

Figure 3: **Correlation of DORT with transfer success after training in veridical feedback group:** To investigate whole-brain neural activity correlating with successful SN/VTA self-regulation, we used DORT as measure of regulation success and correlated it with the contrast ($IMAGINE_REWARD_{transfer}$ - $REST_{transfer}$) - ($IMAGINE_REWARD_{baseline}$ - $REST_{baseline}$) as measure of learning related change in neural activity. A) The analysis revealed task-specific correlations primarily within the cognitive control network (whole brain overview FWE-corrected with $p<.05$ on cluster level, projected to lateral and medial sagittal sections). B) Exemplary correlations within the cognitive control network have been depicted, here in MFG/dlPFC, ACC, Thalamus, and bilateral Temporal Gyrus, to illustrate the association between neural activity with DORT. The correlations are for illustration purposes only without further significance testing to avoid double dipping. The grey shaded area identifies 95 % confidence interval.

			MNI Coordinates		
Region Label	**# voxels**	**t-value**	**x**	**y**	**z**
Cingulate Gyrus, posterior division	895	6.104	-3	-49	7
Middle Frontal Gyrus (dorsolateral prefrontal cortex)	295	4.609	45	31	19
Left Thalamus	1281	4.472	-9	-24	10
Temporal Occipital Fusiform Cortex	715	5.858	32	-46	-22

Lingual Gyrus (Right Parahippocampal Gyrus)	715	3.725	20	-46	-6
Right Cerebral White Matter (Right Hippocampus)	298	5.300	20	-18	-10
Left Hippocampus	408	3.703	-26	-33	-12
Left Cerebral White Matter (Left Middle Occipital Gyrus)	693	5.056	-36	-73	31
Left Cerebral White Matter (Left Superior Medial Gyrus, Anterior Cingulate Cortex)	579	4.960	-9	28	38
Intracalcarine Cortex (Right Lingual Gyrus)	856	4.048	6	-82	1
Occipital Fusiform Gyrus	474	4.928	29	-66	-12
Middle Temporal Gyrus (Left Inferior Temporal Gyrus)	1028	4.913	-62	-37	-16
Middle Temporal Gyrus (Left Inferior Temporal Gyrus)	1028	4.315	-59	-57	-3
Occipital Fusiform Gyrus	658	4.866	-42	-70	-19
Temporal Fusiform Cortex, posterior division	658	4.638	-39	-43	-28
Temporal Occipital Fusiform Cortex	658	4.401	-23	-66	-19
Superior Frontal Gyrus	310	4.736	6	2	80
Central Opercular Cortex (Left Superior Temporal Gyrus)	309	4.636	-59	-16	16
Left Cerebral White Matter (Left inferior Frontal Gyrus)	401	4.589	-39	35	-9
Location not in atlas	408	4.578	-14	-49	-22
Location not in atlas (Right Paracentral Lobule)	341	5.003	2	-39	82
Location not in atlas (Left Cerebellum IV)	856	4.947	-6	-66	-15

Table 1 Correlation of transfer activity ($IMAGINE_REWARD_{transfer}$ - $REST_{transfer}$) - ($IMAGINE_REWARD_{baseline}$ - $REST_{baseline}$) with DORT in veridical feedback group (see Figure 3a). Table shows all local maxima separated by more than 20 mm; for all clusters, $p < 0.05$ FWE-corrected on cluster level, $t > 3.30$; $p < 0.001$; $df = 40$. Regions were labelled using the Harvard-Oxford atlas and/or the Anatomy Toolbox in parentheses; the activity in SN/VTA has been excluded from the table to avoid circularity; x,y,z = Montreal Neurological Institute (MNI) coordinates in the left-right, anterior-posterior, and inferior-superior dimensions, respectively.

3.2.2 Inverted feedback group

For the inverted feedback group, the same analysis resulted in partly distinct activations. In contrast to the veridical feedback group, left amygdala activity correlated significantly with DORT (Fig. 4 and Table S2). Importantly, activity in cognitive control areas reported above, such as dlPFC and ACC, was significantly weaker in inverted than veridical feedback groups (Table S3 for disjunction and direct statistical comparison). These regions therefore appear to play a preferential role for successful transfer of SN/VTA self-regulation.

We also tested for common activity in the two feedback groups using conjunction analysis. Similar to the veridical group, the inverted feedback group showed correlations between DORT and activity in the precuneus, middle temporal gyrus, insula, IFG, thalamus, and parahippocampal gyrus (Table S4). These common areas appear to reflect non-specific regulation activity and may be associated with memory and introspection processes.

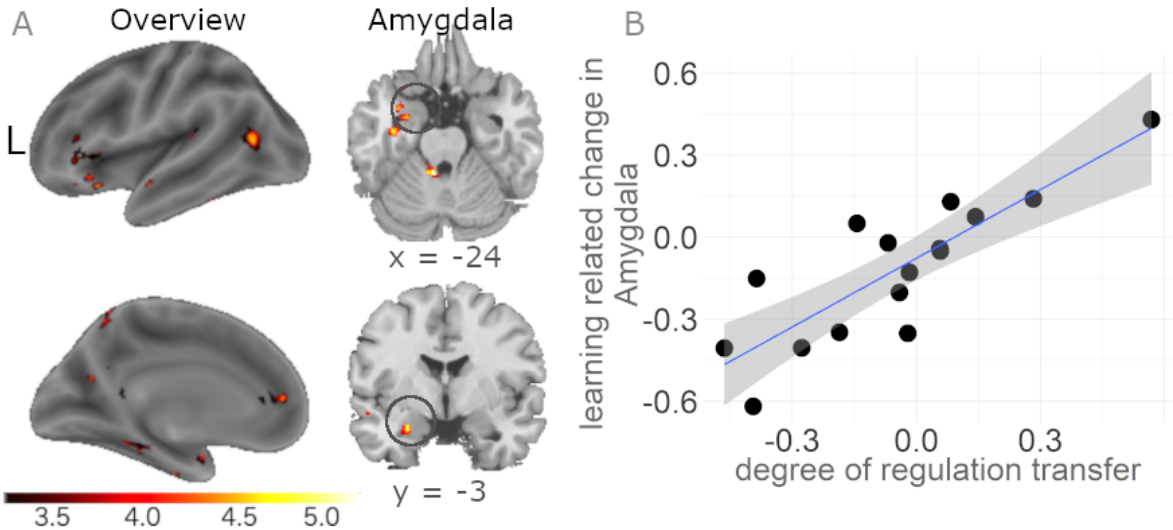

Figure 4 **Correlation of DORT with transfer success after training in inverted feedback group:** (A) Receiving inverted feedback resulted in a correlation between DORT as measure of regulation success and the contrast ($IMAGINE_REWARD_{transfer}$ - $REST_{transfer}$) - ($IMAGINE_REWARD_{baseline}$ - $REST_{baseline}$) as measure of learning related change in the amygdala ($p<.001$). This region was not observed in the veridical group. (B) The correlation depicts the positive association of neural activity in the amygdala with DORT. The plot is for illustration purposes only without further significance testing to avoid double dipping. The grey shaded area identifies the 95 % confidence interval.

3.3 Reinforcement learning: DLPFC prediction error coding during neurofeedback training correlates with DORT

To investigate whether reinforcement learning mechanisms contribute to successful neurofeedback transfer, we tested for time-resolved parametric prediction error related activity during the training runs. We reasoned that prediction error activity should decrease from early to late phases of neurofeedback training for successful regulators. At any time during neurofeedback training, participants needed to come up with their own predictions of the upcoming feedback signal and compare the predictions with actual feedback at the next time point. Similarly, in temporal difference learning models, prediction errors are calculated at each moment in time (Sutton and Barto, 2018). Therefore, we operationalized prediction error by subtracting the immediately preceding SN/VTA activity (prediction) from the present SN/VTA activity (outcome). This analysis revealed that prediction

328 error signals in dlPFC decreased with ongoing neurofeedback training only for participants with high
329 DORT (Fig. 5). To assess this finding in more detail, we also analysed the two neurofeedback training
330 runs separately. This analysis confirmed that more successful participants showed more pronounced
331 dlPFC coding of prediction error in early compared to later training (see Fig. S3 for run-wise PE coding
332 in dlPFC).

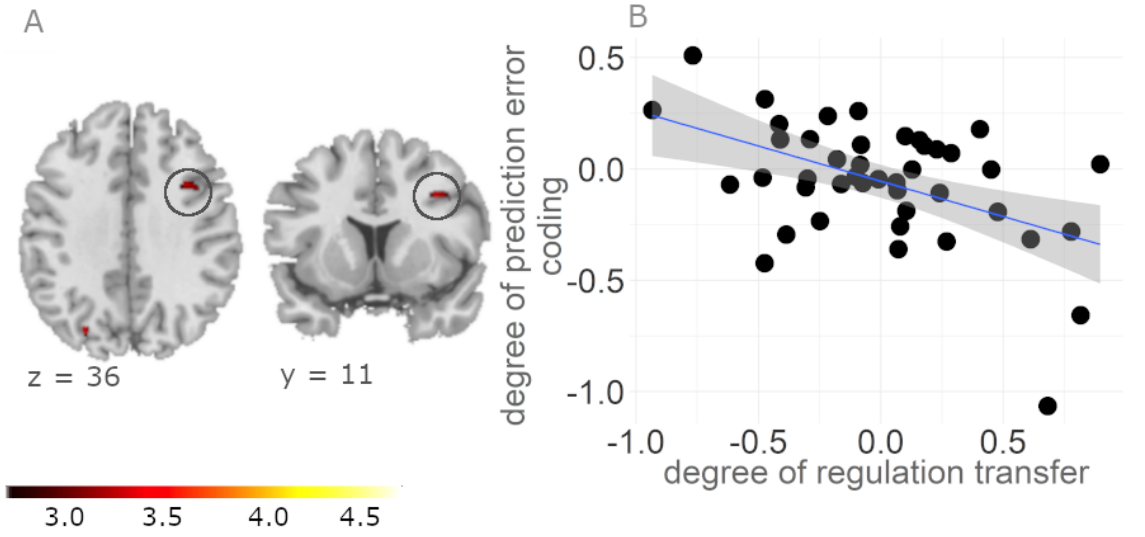

Figure 5: **Prediction error coding in dlPFC decreases during NF training in participants with successful SN/VTA self-regulation:** (A) The time-resolved neural prediction error signal, corresponding to the parametric difference between the current and immediately preceding feedback activity from the SN/VTA decreased with ongoing feedback training within dlPFC as a function of degree of regulation transfer (p<.001). This finding is consistent with reinforcement learning theories, according to which prediction errors decrease as learning progresses. By extension, reinforcement learning mechanisms can explain successful neurofeedback training. (B) The plot depicts correlation of neural activity in the dlPFC with DORT. The plot is for illustration purposes only without further significance testing to avoid double dipping. The grey shaded area identifies the 95 % confidence interval.

333 **3.4 Learning-related functional coupling of DLPFC with SN/VTA**

334 Our finding of time-resolved prediction error coding in dlPFC inspired a complementary functional
335 connectivity analysis. We used the prediction error coding area within the dlPFC as a seed region to
336 investigate coupling to the SN/VTA region our participants aimed to regulate. Functional connectivity
337 between the two regions increased with transfer success (Fig. 6; (t(40) = 3.79, cluster extent = 16, MNI
338 x = -2, y = -16, z = -15). In other words, DORT and dlPFC to SN/VTA connectivity correlated positively.
339 Note that this correlation of DORT with dlPFC-SN/VTA connectivity was task-related as it was enhanced
340 during IMAGINE_REWARD relative to REST (which served as psychological regressor) and independent
341 of SN/VTA activity.

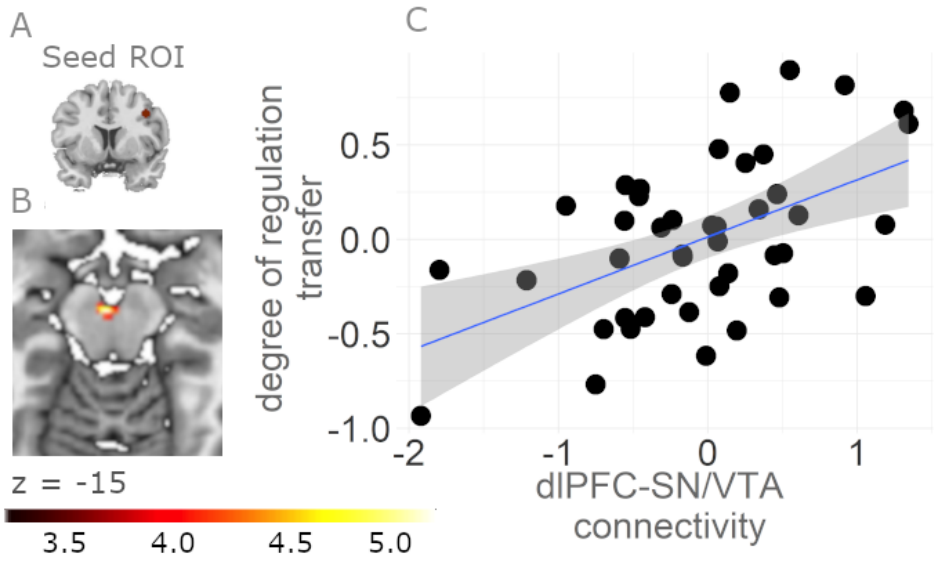

Figure 6 **Functional connectivity between dlPFC and SN/VTA correlates with transfer success:** (A) A functional connectivity analysis based on the prediction error coding seed region in the dlPFC (MNI coordinate 40, 10, 38, 5 cm sphere) revealed that increasing connectivity to the SN/VTA correlated with increasing success of neurofeedback training (p<.001). (B) DORT increased with increasing connectivity between dlPFC and SN/VTA during IMAGINE_REWARD vs. REST in neurofeedback training runs. Thus, dlPFC appears to regulate SN/VTA in proportion to the degree to which neurofeedback training is successful. (C) The correlation plot depicts connectivity between dlPFC and SN/VTA with DORT. The plot is for illustration purposes only without further significance testing to avoid double dipping. The grey shaded area identifies the 95 % confidence interval.

3.5 Individual differences in dlPFC reward sensitivity during MID task correlate with regulation success

In Study 2 we used the MID task to independently measure reward sensitivity and the capability to adapt to different reward contexts (Kirschner et al., 2018a). We asked whether individual measures of reward processing (measured with parametric and adaptive coding of reward related BOLD activity) are predictive for individual regulation. Specifically, we tested for correlations between DORT and MID reward sensitivity (sum of small and large reward parametric modulators) and MID adaptive reward coding (difference of small minus large reward parametric modulators). A conjunction of three correlations with DORT – reward sensitivity in the MID task, adaptive reward coding in the MID task and the contrast ($IMAGINE_REWARD_{transfer}$ - $REST_{transfer}$) - ($IMAGINE_REWARD_{baseline}$ - $REST_{baseline}$) outside SN/VTA revealed common neural activity in the dlPFC (center at MNI x = 40, y = 10, z = 38; Fig. 7 and Table S6). Thus, the more successful individuals were at self-regulating SN/VTA as a result of

355 neurofeedback training, the more sensitive they were to reward and the more strongly they adapted

356 to different reward contexts in the MID task.

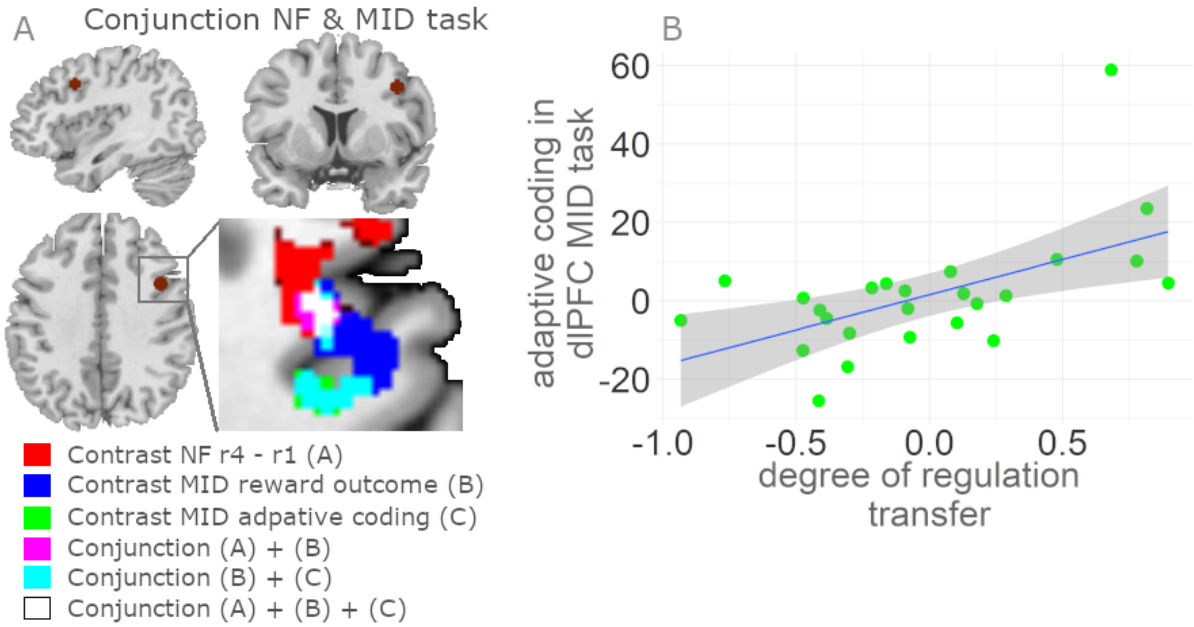

Figure 7 **Reward-sensitivity in dlPFC correlates with successful SN/VTA self-regulation**: (A) SN/VTA DORT in the neurofeedback task correlated with prefrontal reward sensitivity and adaptive coding in the MID task. A conjunction analysis around the peak coordinate in dlPFC showing prediction error coding during neurofeedback training (MNI x = 40, y = 10, z = 38, left) revealed common neural activity reflecting transfer ($IMAGINE_REWARD_{transfer}$ - $REST_{transfer}$) - ($IMAGINE_REWARD_{baseline}$ - $REST_{baseline}$) and reward sensitivity (small + large reward magnitude parametric modulators in MID, all contrasts with p<.001). Moreover, individuals with more successful self-regulation of the SN/VTA showed stronger adaptive coding (which reflects higher sensitivity to small relative to large rewards) in the same region that also showed learning-related decreases in prediction error coding during neurofeedback training (right). (B) The correlation plot depicts the adaptive coding activity in dlPFC with DORT. The plot is for illustration purposes only without further significance testing to avoid double dipping. The grey shaded area identifies the 95 % confidence interval.

357 # 4 Discussion

358 In the present work, we used data acquired from two previous rt-fMRI neurofeedback studies to

359 characterize individual differences and mechanisms in successfully transferred self-regulation of the

360 dopaminergic midbrain after neurofeedback training. We found a strong relation between self-

361 regulation success and increases in post-training activity in the cognitive control network. Moreover,

362 we found four correlations with increasing transfer effects: (i) decreasing dlPFC prediction error signals

363 during neurofeedback training, (ii) increasing connectivity of dlPFC to the SN/VTA for reward

364 imagination compared to rest during transfer, (iii) increasing reward sensitivity in dlPFC and (iv)

365 increasing adaptive reward coding in dlPFC in the independent MID task. Together, our study

elucidates the mechanistic control of the dopaminergic midbrain via the cognitive control network and suggests that reinforcement learning contributes to successful neurofeedback training.

Sustained self-regulation skills and the generalization of learning after neurofeedback training are key elements for practical applications and remain one of the major challenges in rt-FMRI neurofeedback research (Sulzer et al., 2013a). Results from previous neurofeedback studies of the reward system have been inconclusive (Greer et al., 2014; Kirschner et al., 2017; Sulzer et al., 2013b) and only one study (MacInnes et al., 2016) reported significant post-training activity in the VTA, and increased mesolimbic network connectivity. Methodological limitations might have hampered the ability to detect transfer effects. First, previous studies focused exclusively on self-regulation of one *a priori* target region, such as SN/VTA, instead of investigating large-scale post-training effects within the whole brain. Second, transfer effects were examined at the group-level, which did not reflect the individual learning success. In the present study we overcome both limitations by taking advantage of an individual measure of transfer success (DORT) and focusing on the whole brain.

One insight of the present study is that transfer success associates with neural activity in cognitive control network areas (Niendam et al., 2012; Parro et al., 2018), such as dlPFC and ACC. This network overlaps with regions that have been associated with feedback-related information processing during training (Marco-Pallarés et al., 2007, Emmert et al., 2016). Together, these findings suggest that the same regions contribute to acquisition and transfer of neurofeedback and that sustained post-training self-regulation generalizes across a functional network of different brain regions. Intriguingly, similar networks have been reported in skill learning. Future studies might investigate commonalities between neurofeedback and particularly cognitive skill learning, taking into account the specific temporal dynamics of both functions (Birbaumer et al., 2013; Tenison et al., 2016).

The finding that individuals with more successful regulation of the dopaminergic midbrain show stronger activation of cognitive control areas during transfer speaks to our understanding of how individual differences in cognitive control affect emotion regulation (Braver et al., 2010; Buhle et al.,

391 2014; Friedman and Miyake, 2017; Kohn et al., 2014). For example the working memory component
392 of cognitive control has been shown to predict negative affect reduction through reappraisal and
393 suppression (Hendricks and Buchanan, 2016) Interestingly, dopamine action (particularly at D1
394 receptors) in dlPFC sustains working memory performance (Arnsten et al., 2015). Thus, it is conceivable
395 that frontolimbic loops contribute to successful transfer.

396 Although speculative at this point, the positive post-training effects on the cognitive-control network
397 activity might also have implications for transdiagnostic clinical applications. First, combining rt-fMRI
398 neurofeedback training with different forms of psychotherapy such as cognitive behavioral therapy
399 (Beck, 2005), dialectical behavioral therapy (Lynch et al., 2007), or psychodynamic therapy (Bateman
400 and Fonagy, 2010; Have-de Labije and Neborsky, 2012; Maroda, 2010) could improve emotion
401 regulation deficits prevalent in several psychiatric disorders including substance use disorders,
402 depression, anxiety and personality disorders. With particular attention to substance use disorders,
403 maladaptive changes in neuroplasticity within the cognitive control network are closely associated
404 with loss of control and compulsive drug-seeking (George and Koob, 2010; Holmes et al., 2016; Koob
405 and Volkow, 2010). In these patients, neurofeedback training might be able to directly target the
406 biological correlates and reinstate function of the cognitive-control network.

407 We found stronger reductions in prediction error coding in the DLPFC for regulators than non-
408 regulators. This finding suggests that prediction error-driven reinforcement learning was more
409 pronounced in regulators than non-regulators and provides empirical evidence for previous theoretical
410 proposals on the mechanisms of neurofeedback learning independent of feedback modality
411 (Birbaumer et al., 2013). Thus, reinforcement learning mechanisms provide a framework for
412 understanding how neurofeedback works. Future research may want to investigate whether the rich
413 theoretical and empirical tradition of reinforcement learning, (e.g. Pearce, 2008), can be harnessed to
414 facilitate neurofeedback training.

415 We found that successful SN/VTA self-regulation is associated with an increased functional coupling
416 between dlPFC regions coding prediction error and the dopaminergic midbrain. This coupling fits well
417 with anatomical connections between dlPFC and the dopaminergic midbrain (Frankle et al., 2006;
418 Sesack et al., 2003) as well as functional connectivity studies on motivation (Ballard et al., 2011) and
419 animal studies on prefrontal regulation of midbrain activity (Gao et al., 2007; Jo and Mizumori, 2016).
420 The animal work suggests that prefrontal cortex controls dopaminergic neurons primarily indirectly,
421 through inhibitory relay neurons. By showing top-down control of the midbrain, our data go beyond
422 previous connectivity studies of the dopamine system, which primarily focused on coupling between
423 the prefrontal cortex and the striatum (Chatham et al., 2014; Schenk et al., 2017; Weber et al., 2018).

424 At the functional level, a recent study on creative problem solving in humans highlights that dlPFC is
425 involved in experiencing a moment of insight, the so called Aha!-moment (Tik et al., 2018). According
426 to this effective connectivity study, dlPFC could upregulate the VTA/SN via striatal connections during
427 such a moment. On the other hand, in trials where no solution was found for a given problem, also no
428 significant connectivity was observed. This study supports our finding that dlPFC-SN/VTA connectivity
429 plays an important role in self-guided motivation and in internal reward processing. Our finding
430 highlights that cognitive and affective mechanisms associated with different experiences also involve
431 different neural pathways. Future studies should investigate to what degree individual differences in
432 the functional architecture of brain networks (Hahn et al., 2014) influence these internal reward
433 mechanisms and to which degree different strategies can influence neurofeedback training success.

434 Our independent reward task revealed that individual differences in prefrontal reward sensitivity and
435 efficient adaptive reward coding were associated with successful SN/VTA self-regulation. Adaptive
436 coding of rewards captures the notion that neural activity (output) should match the most likely inputs
437 to maximize efficiency and representational precision (Wark et al., 2007). Accordingly, we previously
438 showed that reward regions encode a small range of rewards more strongly than the large range of
439 rewards (Kirschner et al., 2018a, 2016). Interestingly, participants who were more sensitive to small
440 rewards were also more successful in self-regulation of the dopaminergic midbrain in the present

441 study. When participants in a typical neurofeedback training paradigm succeed at increasing the
442 activity of the self-regulated area, the ensuing change in visual stimulation (positive neurofeedback)
443 may constitute a small reward. By extension, adaptive reward coding may therefore provide a useful
444 handle on identifying regulators. Moreover, future neurofeedback experiments should consider
445 scaling the feedback signal to avoid sensitivity limitations, particularly in individuals with reduced
446 adaptive coding.

447 A potential limitation of our study is that we used a combined mask for SN and VTA even though
448 differences in functionality and anatomy have been reported for the two regions (reviewed e.g. in
449 Trutti et al., 2019), with the SN more related to motor functions and the VTA to reward functions.
450 However, it should be kept in mind that when viewed through the lens of recording and imaging rather
451 than lesion techniques the differences are more gradual than categorical (Düzel et al., 2009). Still,
452 future studies may want to use more specific feedback from one or the other region to more
453 specifically target potential differences in functions.

454 5 Conclusions

455 We showed that successful transfer in SN/VTA self-regulation after neurofeedback training is
456 associated with activity in the cognitive control network and dlPFC. Future studies could employ
457 cognitive control activity during neurofeedback training to boost success rates and clinical outcomes.
458 Furthermore, our findings of decreasing prediction error signals in dlPFC suggest that associative
459 learning contributes to real-time fMRI neurofeedback effects. Finally, we show that higher individual
460 reward sensitivity increases the chance of neurofeedback training success. Patients with reduced
461 reward sensitivity may therefore benefit from careful scaling of the neurofeedback information.

Acknowledgments

The authors would like to thank Silvia Maier and Stephan Nebe for comments on previous versions of the manuscript and fruitful discussions.

This project was supported by the European Union's Horizon 2020 research and innovation program under the Grant Agreement No 794395 (to LH) and grant 100014_165884 from the Swiss National Science Foundation (to PT). MK received grant support from the National Bank Fellowship (McGill) and Swiss National Science Foundation (P2SKP3_178175).

The authors declare no competing financial interests.

References

Alkoby, O., Abu-Rmileh, A., Shriki, O., Todder, D., 2018. Can We Predict Who Will Respond to Neurofeedback? A Review of the Inefficacy Problem and Existing Predictors for Successful EEG Neurofeedback Learning. Neuroscience 378, 155–164. https://doi.org/10.1016/J.NEUROSCIENCE.2016.12.050

Arnsten, A.F.T., Wang, M., Paspalas, C.D., 2015. Dopamine's Actions in Primate Prefrontal Cortex: Challenges for Treating Cognitive Disorders. Pharmacol. Rev. 67, 681–696. https://doi.org/10.1124/pr.115.010512

Ballard, I.C., Murty, V.P., Carter, R.M., MacInnes, J.J., Huettel, S.A., Adcock, R.A., 2011. Dorsolateral Prefrontal Cortex Drives Mesolimbic Dopaminergic Regions to Initiate Motivated Behavior. J. Neurosci. 31, 10340–10346. https://doi.org/10.1523/jneurosci.0895-11.2011

Bateman, A., Fonagy, P., 2010. Mentalization based treatment for borderline personality disorder. World Psychiatry 9, 11–5.

Beck, A.T., 2005. The current state of cognitive therapy: A 40-year retrospective. Arch. Gen. Psychiatry. https://doi.org/10.1001/archpsyc.62.9.953

Birbaumer, N., Ruiz, S., Sitaram, R., 2013. Learned regulation of brain metabolism. Trends Cogn. Sci. 17, 295–302. https://doi.org/10.1016/j.tics.2013.04.009

Braver, T.S., Cole, M.W., Yarkoni, T., 2010. Vive les differences! Individual variation in neural mechanisms of executive control. Curr. Opin. Neurobiol. https://doi.org/10.1016/j.conb.2010.03.002

Bromberg-Martin, E.S., Matsumoto, M., Hikosaka, O., 2010. Dopamine in Motivational Control: Rewarding, Aversive, and Alerting. Neuron. https://doi.org/10.1016/j.neuron.2010.11.022

Buhle, J.T., Silvers, J.A., Wage, T.D., Lopez, R., Onyemekwu, C., Kober, H., Webe, J., Ochsner, K.N., 2014. Cognitive reappraisal of emotion: A meta-analysis of human neuroimaging studies. Cereb. Cortex 24, 2981–2990. https://doi.org/10.1093/cercor/bht154

Burke, C.J., Tobler, P.N., 2016. Time, Not Size, Matters for Striatal Reward Predictions to Dopamine. Neuron. https://doi.org/10.1016/j.neuron.2016.06.029

Chatham, C.H., Frank, M.J., Badre, D., 2014. Corticostriatal output gating during selection from working memory. Neuron 81, 930–942. https://doi.org/10.1016/j.neuron.2014.01.002

Deserno, L., Schlagenhauf, F., Heinz, A., 2016. Striatal dopamine, reward, and decision making in schizophrenia. Dialogues Clin. Neurosci. 18, 77–89.

Düzel, E., Bunzeck, N., Guitart-Masip, M., Wittmann, B., Schott, B.H., Tobler, P.N., 2009. Functional imaging of the human dopaminergic midbrain. Trends Neurosci. 32, 321–328. https://doi.org/10.1016/j.tins.2009.02.005

Emmert, K., Kopel, R., Koush, Y., Maire, R., Senn, P., De Ville, D. Van, Haller, S., 2017. Continuous vs. intermittent neurofeedback to regulate auditory cortex activity of tinnitus patients using real-time fMRI - A pilot study. NeuroImage Clin. 14, 97–104. https://doi.org/10.1016/j.nicl.2016.12.023

Frankle, W.G., Laruelle, M., Haber, S.N., 2006. Prefrontal cortical projections to the midbrain in primates: Evidence for a sparse connection. Neuropsychopharmacology 31, 1627–1636.

https://doi.org/10.1038/sj.npp.1300990

Friedman, N.P., Miyake, A., 2017. Unity and diversity of executive functions: Individual differences as a window on cognitive structure. Cortex. https://doi.org/10.1016/j.cortex.2016.04.023

Friston, K., Schwartenbeck, P., FitzGerald, T., Moutoussis, M., Behrens, T., Dolan, R.J., 2014. The anatomy of choice: Dopamine and decision-making. Philos. Trans. R. Soc. B Biol. Sci. 369. https://doi.org/10.1098/rstb.2013.0481

Gao, M., Liu, C.-L., Yang, S., Jin, G.-Z., Bunney, B.S., Shi, W.-X., 2007. Functional Coupling between the Prefrontal Cortex and Dopamine Neurons in the Ventral Tegmental Area. J. Neurosci. 27, 5414–5421. https://doi.org/10.1523/jneurosci.5347-06.2007

George, O., Koob, G.F., 2010. Individual differences in prefrontal cortex function and the transition from drug use to drug dependence. Neurosci. Biobehav. Rev. https://doi.org/10.1016/j.neubiorev.2010.05.002

Greer, S.M., Trujillo, A.J., Glover, G.H., Knutson, B., 2014. Control of nucleus accumbens activity with neurofeedback. Neuroimage 96, 237–244. https://doi.org/10.1016/j.neuroimage.2014.03.073

Hahn, A., Kranz, G.S., Sladky, R., Ganger, S., Windischberger, C., Kasper, S., Lanzenberger, R., 2014. Individual Diversity of Functional Brain Network Economy. Brain Connect. 5, 156–165. https://doi.org/10.1089/brain.2014.0306

Have-de Labije, J., Neborsky, R., 2012. Mastering intensive short-term dynamic psychotherapy: a roadmap to the unconscious. Karnac Books, London.

Hendricks, M.A., Buchanan, T.W., 2016. Individual differences in cognitive control processes and their relationship to emotion regulation. Cogn. Emot. 30, 912–924. https://doi.org/10.1080/02699931.2015.1032893

Holmes, A.J., Hollinshead, M.O., Roffman, J.L., Smoller, J.W., Buckner, R.L., 2016. Individual Differences in Cognitive Control Circuit Anatomy Link Sensation Seeking, Impulsivity, and Substance Use. J. Neurosci. 36, 4038–4049. https://doi.org/10.1523/jneurosci.3206-15.2016

Huys, Q.J.M., Tobler, P.N., Hasler, G., Flagel, S.B., 2014. The role of learning-related dopamine signals in addiction vulnerability, in: Progress in Brain Research. pp. 31–77. https://doi.org/10.1016/B978-0-444-63425-2.00003-9

Jo, Y.S., Mizumori, S.J., 2016. Prefrontal Regulation of Neuronal Activity in the Ventral Tegmental Area. Cereb. Cortex 26, 4057–4068. https://doi.org/10.1093/cercor/bhv215

Kirschner, M., Hager, O.M., Bischof, M., Hartmann, M.N., Kluge, A., Seifritz, E., Tobler, P.N., Kaiser, S., 2016. Ventral striatal hypoactivation is associated with apathy but not diminished expression in patients with schizophrenia. J. Psychiatry Neurosci. 41, 152–161. https://doi.org/10.1503/jpn.140383

Kirschner, M., Haugg, A., Manoliu, A., Simon, J.J., Huys, Q.J.M., Seifritz, E., Tobler, P.N., Kaiser, S., 2018a. Deficits in context-dependent adaptive coding in early psychosis and healthy individuals with schizotypal personality traits. Brain 141, 2806–2819. https://doi.org/10.1093/brain/awy203

Kirschner, M., Haugg, A., Manoliu, A., Simon, J.J., Huys, Q.J.M., Seifritz, E., Tobler, P.N., Kaiser, S., 2018b. Deficits in context-dependent adaptive coding in early psychosis and healthy individuals with schizotypal personality traits. Brain 141, 2806–2819. https://doi.org/10.1093/brain/awy203

Kirschner, M., Sladky, R., Haugg, A., Staempfli, P., Jehli, E., Hodel, M., Engeli, E., Hoesli, S., Baumgartner,

M.R., Sulzer, J., Huys, Q.J.M., Seifritz, E., Quednow, B.B., Scharnowski, F., Herdener, M., 2018c. Self-regulation of the Dopaminergic Reward Circuit in Cocaine Users with Mental Imagery and Neurofeedback. bioRxiv.

Kirschner, M., Stämpfli, P., Jehli, E., Hodel, M., Engeli, E., Hulka, L., Scharnowski, F., Sulzer, J., Seifritz, E., Quednow, B., Herdener, M., 2017. Self-regulation and real time fMRI neurofeedback of the dopaminergic reward system in cocaine users Background & Objectives Key findings. Proc. Annu. Meet. Soc. Biol. Psychiatry 8001.

Klein, M.O., Battagello, D.S., Cardoso, A.R., Hauser, D.N., Bittencourt, J.C., Correa, R.G., 2019. Dopamine: Functions, Signaling, and Association with Neurological Diseases. Cell. Mol. Neurobiol. 39, 31–59. https://doi.org/10.1007/s10571-018-0632-3

Kohn, N., Eickhoff, S.B., Scheller, M., Laird, A.R., Fox, P.T., Habel, U., 2014. Neural network of cognitive emotion regulation - An ALE meta-analysis and MACM analysis. Neuroimage 87, 345–355. https://doi.org/10.1016/j.neuroimage.2013.11.001

Koob, G.F., Volkow, N.D., 2010. Neurocircuitry of addiction. Neuropsychopharmacology 35, 217–38. https://doi.org/10.1038/npp.2009.110

Krohne, H.W., Egloff, B., Kohlmann, C.-W., Tausch, A., 1996. Untersuchung mit einer deutschen Form der Positive and Negative Affect Schedule (PANAS). Diagnostica 42, 139–156.

Lehrl, S., 2005. Mehrfachwahl-Wortschatz-Intelligenztest MWT-B., 5th ed. Spitta Verlag, Balingen.

Lynch, T.R., Trost, W.T., Salsman, N., Linehan, M.M., 2007. Dialectical Behavior Therapy for Borderline Personality Disorder. Annu. Rev. Clin. Psychol. 3, 181–205. https://doi.org/10.1146/annurev.clinpsy.2.022305.095229

MacInnes, J.J., Dickerson, K.C., Chen, N. kuei, Adcock, R.A., 2016. Cognitive Neurostimulation: Learning to Volitionally Sustain Ventral Tegmental Area Activation. Neuron 89, 1331–1342. https://doi.org/10.1016/j.neuron.2016.02.002

Maia, T. V., Frank, M.J., 2017. An Integrative Perspective on the Role of Dopamine in Schizophrenia. Biol. Psychiatry 81, 52–66. https://doi.org/10.1016/j.biopsych.2016.05.021

Marco-Pallarés, J., Müller, S.V., Münte, T.F., 2007. Learning by doing: An fMRI study of feedback-related brain activations. Neuroreport 18, 1423–1426. https://doi.org/10.1097/WNR.0b013e3282e9a58c

Maroda, K.J., 2010. Psychodynamic Techniques: Working with Emotion in the Therapeutic Relationship, Journal of Phenomenological Psychology. Guilford Press, New York, US. https://doi.org/10.1163/156916211x567505

McLaren, D.G., Ries, M.L., Xu, G., Johnson, S.C., 2012. A generalized form of context-dependent psychophysiological interactions (gPPI): A comparison to standard approaches. Neuroimage 61, 1277–1286. https://doi.org/10.1016/j.neuroimage.2012.03.068

Meder, D., Herz, D.M., Rowe, J.B., Lehéricy, S., Siebner, H.R., 2019. The role of dopamine in the brain - lessons learned from Parkinson's disease. Neuroimage 190, 79–93. https://doi.org/10.1016/j.neuroimage.2018.11.021

Miyapuram, K.P., Tobler, P.N., Gregorios-Pippas, L., Schultz, W., 2012. BOLD responses in reward regions to hypothetical and imaginary monetary rewards. Neuroimage 59, 1692–1699. https://doi.org/10.1016/j.neuroimage.2011.09.029

Murty, V.P., Shermohammed, M., Smith, D. V, Carter, R.M., Huettel, S.A., Adcock, R.A., 2014. Resting state networks distinguish human ventral tegmental area from substantia nigra. Neuroimage 100, 580–9. https://doi.org/10.1016/j.neuroimage.2014.06.047

Niendam, T.A., Laird, A.R., Ray, K.L., Dean, Y.M., Glahn, D.C., Carter, C.S., 2012. Meta-analytic evidence for a superordinate cognitive control network subserving diverse executive functions. Cogn. Affect. Behav. Neurosci. 12, 241–68. https://doi.org/10.3758/s13415-011-0083-5

Oblak, E.F., Lewis-Peacock, J.A., Sulzer, J.S., 2017. Self-regulation strategy, feedback timing and hemodynamic properties modulate learning in a simulated fMRI neurofeedback environment. PLoS Comput. Biol. 13, e1005681. https://doi.org/10.1371/journal.pcbi.1005681

Parro, C., Dixon, M.L., Christoff, K., 2018. The neural basis of motivational influences on cognitive control. Hum. Brain Mapp. 39, 5097–5111. https://doi.org/10.1002/hbm.24348

Pearce, J., 2008. Animal Learning and Cognition: An Introduction, 3rd ed.

Preuss, U.W., Rujescu, D., Giegling, I., Watzke, S., Koller, G., Zetzsche, T., Meisenzahl, E.M., Soyka, M., Möller, H.J., 2008. Psychometrische evaluation der deutschsprachigen version der Barratt-Impulsiveness-Skala. Nervenarzt 79, 305–319. https://doi.org/10.1007/s00115-007-2360-7

Radua, J., Stoica, T., Scheinost, D., Pittenger, C., Hampson, M., 2018. Neural Correlates of Success and Failure Signals During Neurofeedback Learning. Neuroscience 378, 11–21. https://doi.org/10.1016/j.neuroscience.2016.04.003

Schenk, L.A., Sprenger, C., Onat, S., Colloca, L., Büchel, C., 2017. Suppression of Striatal Prediction Errors by the Prefrontal Cortex in Placebo Hypoalgesia. J. Neurosci. 37, 9715–9723. https://doi.org/10.1523/jneurosci.1101-17.2017

Schultz, W., 2016. Dopamine reward prediction error coding. Dialogues Clin. Neurosci. 18, 23–32.

Schultz, W., 1998. Predictive Reward Signal of Dopamine Neurons. J. Neurophysiol. 80, 1–27.

Sesack, S.R., Carr, D.B., Omelchenko, N., Pinto, A., 2003. Anatomical Substrates for Glutamate-Dopamine Interactions: Evidence for Specificity of Connections and Extrasynaptic Actions, in: Annals of the New York Academy of Sciences. John Wiley & Sons, Ltd (10.1111), pp. 36–52. https://doi.org/10.1196/annals.1300.066

Simon, J.J., Cordeiro, S.A., Weber, M.A., Friederich, H.C., Wolf, R.C., Weisbrod, M., Kaiser, S., 2015. Reward System Dysfunction as a Neural Substrate of Symptom Expression Across the General Population and Patients with Schizophrenia. Schizophr. Bull. 41, 1370–1378. https://doi.org/10.1093/schbul/sbv067

Sitaram, R., Ros, T., Stoeckel, L., Haller, S., Scharnowski, F., Lewis-Peacock, J., Weiskopf, N., Blefari, M.L., Rana, M., Oblak, E., Birbaumer, N., Sulzer, J., 2016. Closed-loop brain training: the science of neurofeedback. Nat. Rev. Neurosci. 18, 86–100. https://doi.org/10.1038/nrn.2016.164

Sladky, R., Baldinger, P., Kranz, G.S., Tr??stl, J., H??flich, A., Lanzenberger, R., Moser, E., Windischberger, C., 2013. High-resolution functional MRI of the human amygdala at 7 T. Eur. J. Radiol. 82, 728–733. https://doi.org/10.1016/j.ejrad.2011.09.025

Sladky, R., Friston, K.J., Tröstl, J., Cunnington, R., Moser, E., Windischberger, C., 2011. Slice-timing effects and their correction in functional MRI. Neuroimage 58, 588–594. https://doi.org/10.1016/j.neuroimage.2011.06.078

Spunt, B., 2016. Spunt/Bspmview: Bspmview V.20161108. https://doi.org/10.5281/ZENODO.168074

Sulzer, J., Haller, S., Scharnowski, F., Weiskopf, N., Birbaumer, N., Blefari, M.L., Bruehl, A.B., Cohen, L.G., DeCharms, R.C., Gassert, R., Goebel, R., Herwig, U., LaConte, S., Linden, D., Luft, A., Seifritz, E., Sitaram, R., 2013a. Real-time fMRI neurofeedback: Progress and challenges. Neuroimage 76, 386–399. https://doi.org/10.1016/j.neuroimage.2013.03.033

Sulzer, J., Sitaram, R., Blefari, M.L., Kollias, S., Birbaumer, N., Stephan, K.E., Luft, A., Gassert, R., 2013b. Neurofeedback-mediated self-regulation of the dopaminergic midbrain. Neuroimage 75, 176–184. https://doi.org/10.1016/j.neuroimage.2013.02.041

Sutton, R.S., Barto, A.G., 2018. Reinforcement Learning: An Introduction, 2nd ed. A Bradford Book, Cambridge.

Tenison, C., Fincham, J.M., Anderson, J.R., 2016. Phases of learning: How skill acquisition impacts cognitive processing. Cogn. Psychol. 87, 1–28. https://doi.org/10.1016/J.COGPSYCH.2016.03.001

Tik, M., Sladky, R., Luft, C.D.B., Willinger, D., Hoffmann, A., Banissy, M.J., Bhattacharya, J., Windischberger, C., 2018. Ultra-high-field fMRI insights on insight: Neural correlates of the Aha!-moment. Hum. Brain Mapp. 39, 3241–3252. https://doi.org/10.1002/hbm.24073

Tobler, P.N., Fiorillo, C.D., Schultz, W., 2005. Adaptive coding of reward value by dopamine neurons. Science 307, 1642–5. https://doi.org/10.1126/science.1105370

Tobler, P.N., Fletcher, P.C., Bullmore, E.T., Schultz, W., 2007. Learning-Related Human Brain Activations Reflecting Individual Finances. Neuron 54, 167–175. https://doi.org/10.1016/j.neuron.2007.03.004

Trutti, A.C., Mulder, M.J., Hommel, B., Forstmann, B.U., 2019. Functional neuroanatomical review of the ventral tegmental area. Neuroimage. https://doi.org/10.1016/j.neuroimage.2019.01.062

Wark, B., Lundstrom, B.N., Fairhall, A., 2007. Sensory adaptation. Curr. Opin. Neurobiol. 17, 423–9. https://doi.org/10.1016/j.conb.2007.07.001

Weber, S.C., Kahnt, T., Quednow, B.B., Tobler, P.N., 2018. Frontostriatal pathways gate processing of behaviorally relevant reward dimensions. PLoS Biol. 16, e2005722. https://doi.org/10.1371/journal.pbio.2005722

Weissenbacher, A., Kasess, C., Gerstl, F., Lanzenberger, R., Moser, E., Windischberger, C., 2009. Correlations and anticorrelations in resting-state functional connectivity MRI: A quantitative comparison of preprocessing strategies. Neuroimage 47, 1408–1416. https://doi.org/10.1016/j.neuroimage.2009.05.005

Wise, R.A., 2004. Dopamine, learning and motivation. Nat. Rev. Neurosci. https://doi.org/10.1038/nrn1406

Wu, J., Gao, M., Shen, J.X., Shi, W.X., Oster, A.M., Gutkin, B.S., 2013. Cortical control of VTA function and influence on nicotine reward. Biochem. Pharmacol. https://doi.org/10.1016/j.bcp.2013.07.013